

Yap1 Is Required for Endothelial to Mesenchymal Transition of the Atrioventricular Cushion*

Received for publication, January 31, 2014, and in revised form, April 23, 2014. Published, JBC Papers in Press, May 15, 2014, DOI 10.1074/jbc.M114.554584

Hui Zhang[‡], Alexander von Gise^{§¶}, Qiaozhen Liu[‡], Tianyuan Hu[‡], Xueying Tian[‡], Lingjuan He[‡], Wenjuan Pu[‡], Xiuzhen Huang[‡], Liang He[‡], Chen-Leng Cai^{||}, Fernando D. Camargo^{**}, William T. Pu^{†1}, and Bin Zhou^{‡2}

From the [‡]Key Laboratory of Nutrition and Metabolism, Institute for Nutritional Sciences, Shanghai Institutes for Biological Sciences, Graduate School of the Chinese Academy of Sciences, Chinese Academy of Sciences, Shanghai 200031, China, the [§]Department of Cardiology, Boston Children's Hospital, Boston, Massachusetts 02115, the ^{||}Department of Developmental and Regenerative Biology, Center for Molecular Cardiology of the Child Health and Development Institute, the Black Family Stem Cell Institute, Mount Sinai School of Medicine, New York, New York 10029, the ^{**}Department of Stem Cell and Regenerative Biology, Harvard University, Cambridge, Massachusetts 02138, and the [†]Department of Pediatric Cardiology and Intensive Care, MHH-Hannover Medical School, 30669 Hannover, Germany

Background: YAP1 regulates EMT and cell proliferation.

Results: Deletion of YAP1 in endocardial cells reduces EMT of endocardial cells, and causes cardiac cushion defect.

Conclusion: YAP1 is required for cardiac cushion development.

Significance: This is the first *in vivo* genetic evidence for YAP1 function in EMT.

Cardiac malformations due to aberrant development of the atrioventricular (AV) valves are among the most common forms of congenital heart diseases. Normally, heart valve mesenchyme is formed from an endothelial to mesenchymal transition (EMT) of endothelial cells of the endocardial cushions. Yes-associated protein 1 (YAP1) has been reported to regulate EMT *in vitro*, in addition to its known role as a major regulator of organ size and cell proliferation in vertebrates, leading us to hypothesize that YAP1 is required for heart valve development. We tested this hypothesis by conditional inactivation of YAP1 in endothelial cells and their derivatives. This resulted in markedly hypocellular endocardial cushions due to impaired formation of heart valve mesenchyme by EMT and to reduced endocardial cell proliferation. In endothelial cells, TGF β induces nuclear localization of Smad2/3/4 complex, which activates expression of *Snail*, *Twist1*, and *Slug*, key transcription factors required for EMT. YAP1 interacts with this complex, and loss of YAP1 disrupts TGF β -induced up-regulation of *Snail*, *Twist1*, and *Slug*. Together, our results identify a role of YAP1 in regulating EMT through modulation of TGF β -Smad signaling and through proliferative activity during cardiac cushion development.

infancy (1–3). The heart valves originate from swellings in the heart tube known as the endocardial cushions. The atrioventricular (AV)³ cushions initiate regional expansion of extracellular matrix (ECM) from both superior and inferior directions at E9.0 in mouse embryos (4, 5). At E9.5, endocardial cells receive activation signals from myocardium, undergo endothelial to mesenchymal transition (EMT), and migrate into endocardial cushions to form heart valve mesenchyme (6). The AV cushions subsequently develop and mature into the final valvuloseptal structures that separate the four chambered heart and permit unidirectional blood flow. Understanding the molecular mechanisms regulating cardiac cushion formation provides new insights into the pathophysiology of congenital heart diseases involving malformed valves.

Among multiple signaling pathways that regulate cardiac cushion development, TGF β signaling plays a key role in regulating cushion EMT (6). TGF β signaling is initiated when homodimers of ligands (TGF β 1–3) bind to type-I or type-II serine/threonine kinase receptors on cell membranes, initiating phosphorylation of Smad (Smad2, Smad3) transcription factors. Phosphorylated Smad2 and Smad3 complex with the common-mediator Smad4 and accumulate in the nucleus to regulate the transcription of specific genes, in cooperation with other transcription factors, coactivators, and corepressors. Epithelial cells, under the influence of TGF β and other signaling pathways, undergo nuclear reprogramming involving several transcription factors, such as *Snail*, *Twist1*, *Slug*, *ZEB1*, and *ZEB2* (7). One key event in heart valve development is the formation of heart valve mesenchyme. Previous studies using *in vitro* collagen gel explant assay showed that TGF β signaling is essential for endocardial cushion EMT (8–11).

Recent studies showed that the Hippo signaling pathway, initially discovered in *Drosophila*, is a key regulator of cell prolifer-

Abnormal heart valve development accounts for a large proportion of congenital heart disease, a major cause of death in

* This work was supported by National Basic Research Program of China (2013CB945302 and 2012CB945102), National Natural Science Foundation of China (91339104, 31271552, 31222038, 31301188), Chinese Academy of Sciences (Hundred Talents Program and KSCX2-EW-R-09), Shanghai Pujiang Program (11PJ1411400) and Basic Research Key Project (14JC1407400), Organization Department of the CPC Central Committee Bajian Talents Program, AstraZeneca, Sanofi-Aventis Shanghai Institutes for Biological Sciences (SA-SIBS) Fellowship, and Postdoc Fund (SIBS-2013KIP311, China-2013M541561).

¹ Supported by funding from National Institutes of Health R01 HL094683.

² To whom correspondence should be addressed: Chinese Academy of Sciences, Shanghai, 200031 China. Tel.: 86-21-54920974; E-mail: zhoubin@sibs.ac.cn.

³ The abbreviations used are: AV, atrioventricular; EMT, endothelial to mesenchymal transition; YAP, Yes-associated protein; ECM, extracellular matrix; H&E, Hematoxylin and Eosin; HUVEC, human umbilical vein endothelial cell.

YAP1 Function in Cardiac Valve Development

eration and organ size. This highly conserved kinase cascade phosphorylates the transcriptional coactivator Yes-associated protein 1 (YAP1), and restrains its activity. Recent studies showed that YAP1 plays an important role in regulating heart growth and regeneration (12–15). YAP1 loss of function caused lethal myocardial hypoplasia, and gain of function enhanced cell-cycle activity in cardiomyocytes both *in vitro* and in fetal and infant hearts. In addition to regulating proliferation, YAP1 also promotes EMT and enhances *in vitro* invasion in cell lines (16–19). *In vivo*, YAP1 has been reported to be potentially prometastatic in breast cancer and melanoma cells (20). Therefore, in addition to cell proliferation, YAP1 enhances multiple other processes including cellular transformation, migration, and invasion. We therefore hypothesized that YAP1 plays an important role in EMT during AV cushion development.

EXPERIMENTAL PROCEDURES

Animals—Tie2-Cre (21) and YAP1^{fl^{ox}} (22) mice were described previously and bred on a C57BL6 background. These mice were crossed to Rosa26^{mTmG} (23) or Rosa26^{LacZ} (24) reporter mice for lineage tracing of endocardial cells. Tie2-Cre; YAP1^{fl/fl} embryos were produced by crossing Tie2-Cre; YAP1^{fl/+} male mice with YAP1^{fl/fl} female mice. PCR analysis on genomic DNA from yolk sac or tails was used for embryo genotyping. This study was carried out in strict accordance with the guidelines in the Institutional Animal Care and Use Committee (IACUC) of the Institute for Nutritional Sciences, Shanghai Institutes for Biological Sciences, Chinese Academy of Sciences.

In Situ Hybridization—Whole mount *in situ* hybridization was performed as described (25). For *in situ* hybridization on cryosections, dissected embryos were fixed overnight in 4% paraformaldehyde and embedded in optimal cutting temperature compound (OCT, Sakura). Embryos were sectioned at 8- μ m thickness. Slides were digested with protease K, acetylated with triethanolamine, dehydrated, and hybridized overnight with riboprobes. The slides were washed in SSC buffer and treated with ribonucleases at 37°C for 30 min. After incubation with anti-digoxigenin antibody (Roche), the slides were developed with BM purple (Roche) in the dark. Primers used for generating probes were: YAP1, sense (5'-TTCCTGATGGATGGGAGCAAG-3') and antisense (5'-TCTGCGGTTCGGGTCTT-TAG-3'); Msx2, sense (5'-AGGAAGACCAGATGGACCAGACTC-3') and antisense (5'-GAAGA-GATGGACAGGAAGGTGAGAC-3'); Notch1, sense (5'-GGGCTATGAATTTCACCGTGG-3') and antisense (5'-GTCTGACAGTCCTCATCAGCTTGAC-3'); Slug, sense (5'-CAAAACCAGA-GATCCTCACCTCG-3') and antisense (5'-CAAAACCTTCTCCAGAATGTCTGC-3'); Nfatc1, sense (5'-CCCGTCACATTCTGGTCCATAC-3') and antisense (5'-TCCTCACACACCTCTGGCAATAC-3'); Ve-cad, sense (5'-GCCAGAAATGCTAAGTATGTGCTCC-3') and antisense (5'-GGTGAAGTTGCTGTCTCGTTC-3'); TGF β 1, sense (5'-TGGTGAACGGAAGCGCATC-3') and antisense (5'-ACTTGACAGGAGCGCACATC-3').

Histological Analysis, Alcian Blue Staining, and Scanning Electron Microscopy (SE)—Embryos were fixed in 4% paraformaldehyde and processed into paraffin-embedded serial sections using routine procedures. For general morphology,

deparaffinized sections were stained with Hematoxylin and Eosin (H&E) using standard procedures. For Alcian blue staining, tissues from paraffin sections were rehydrated and stained in 3% Alcian blue solution (pH 2.5) for 30 min, washed in tap water and counterstained with nuclear fast red. For SE, embryos were sectioned and dewaxed in xylene, and fixed in 5% acetic acid, 3.7% formaldehyde and 50% ethanol. Then the embryos were dehydrated through a series washes in 50, 60, 70, 80, 90, and 100% ethanol. Liquid carbon dioxide was used for critical point drying. All samples were mounted on stubs and gold sputtered before examination in the scanning electron microscope.

X-gal Staining—X-gal staining was performed as described previously (26). Briefly, embryos were fixed in 2% paraformaldehyde and 0.2% glutaraldehyde in PBS for 30 min, and then re-fixed in LacZ fix solution (0.2% glutaraldehyde, 5 mM EGTA, 100 mM MgCl₂ in PBS) for 30 min. After washing three times for 15 min in LacZ wash buffer containing 2 mM MgCl₂, 0.01% sodium deoxycholate, 0.02% Nonidet P-40 in 100 mM sodium phosphate buffer, embryos were stained for 1 h at 37°C in LacZ staining solution containing 1 mg/ml 5-bromo-4-chloro-3-indolyl β -D-galactopyranoside (X-gal) in LacZ wash buffer. Cryosection was performed after whole mount pictures were taken. Pictures were taken under a Leica M165 FC stereomicroscope or Olympus BX53 microscope.

Quantitative RT-PCR Analysis—AV cushion tissues were dissected from E9.5 embryos and every 3 tissues of the same genotype were collected into one tube. RNA was extracted with Trizol according to manufacturer's protocol (Invitrogen) and converted to cDNA using M-MLV reverse transcriptase (Promega, M170A). For qPCR, SYBR Green qPCR master mix (Applied Biosystems) was used, and cDNA was amplified on a StepOnePlus™ Real-Time PCR System (Applied Biosystems).

AV Cushion Explants Culture—A solution (1 mg/ml) of collagen type I (BD Biosciences 354236) was dispensed into 4-well microculture dishes (NUNC) and allowed to solidify inside a 37°C, 5% CO₂ incubator. Collagen gels were washed several times with Opti-MEM. Subsequently, the wells were filled with Opti-MEM containing 1% rat serum, 1% insulin-transferrin-selenium (ITS, Invitrogen), and antibiotics, and incubated overnight. AV explants were harvested in sterile PBS from E9.5 embryos. Explants were placed with the endocardium facing downwards and allowed to attach for 5 h at 37°C, 5% CO₂. DMEM containing 10% FBS and antibiotics was added, and the cultures were incubated for up to 3 days.

Immunostaining and TUNEL Staining—Embryos were collected in PBS on ice and then fixed in 4% paraformaldehyde at 4°C for 30 min. After washing in PBS, embryos were treated with 30% sucrose until fully penetrated. Subsequently, embryos were embedded in OCT and snap frozen. Cryosections of 6–10 μ m thickness were collected on slides. Tissues were blocked with PBS containing 0.1% Triton X-100 and 5% normal donkey serum (PBSST) for 1 h at room temperature, followed by first antibody incubation at 4°C for overnight. Signals were developed with Alexa Fluor secondary antibodies. Before mounting, tissues were counterstained with DAPI. Cultured cells were fixed in 4% paraformaldehyde for 10 min, washed in PBS, and blocked with PBSST for 30 min at room temperature. They

were then stained as described for tissues. Antibodies were used as listed: pHH3 (Upstate, 06-570), Smad2/3 (BD, 610842), p-Smad1/5/8 (CST, 9511), Ki67 (lab vision, RM-9106-F1), TGF β 1 (Santa Cruz Biotechnology, sc-146), NOTCH1 (Santa Cruz Biotechnology, sc-6014-R), GATA4 (R&D, AF2606), p-SMAD2/3 (CST, 9510). For TUNEL staining, the In Situ Cell Death Detection Kit (Roche, 12156792910) was used according to the manufacturer's instruction. Briefly, fixed sections were permeabilized with Triton X-100, followed by PBS wash. The labeling reaction was performed at 37 °C for 60 min by addition of reaction buffer containing enzyme. Images were acquired on a Zeiss LSM510 confocal microscope.

Lentivirus Transfection, Cell Motility Assay, and Luciferase Reporter Assay—Plasmids for packing lentivirus to knock down YAP1 were generated first. Lentivirus was then packaged using HEK293T cells in 60-mm dishes according to Addgene protocol. For the cell motility assay, after lentivirus transduction for 24 h, HUVEC cells plated in a 6-well dish were selected by puromycin at a concentration of 0.5–1 μ g/ml for 3 days. Then the cells were scratched with a 10 μ l pipette tip and treated with or without TGF β 1 (2 ng/ml) in DMEM containing no FBS for 12 h. For luciferase reporter assays, HEK293T cells plated in 24-well dishes at low density were infected with lentivirus and then selected by puromycin at a concentration of 2 μ g/ml for 2 days. Then the cells were transfected with plasmids using calcium phosphate-mediated transfection. After transfection, the cells were serum-starved with or without TGF β 1 (2 ng/ml) treatment for 16 h. We used a Luciferase assay kit (Promega, E1910) to measure the luciferase activity with a luminometer (Berthold Technologies, Bad Wildbad, Germany). Reporter activity was normalized to co-transfected *Renilla*. Plasmids for overexpression of constitutively active Alk5 (ca-Alk5) were gifts from Dr. Yan Chen.

Immunoprecipitation, Western Blotting, ChIP-PCR, and ChIP-qPCR—HUVECs were cultured in DMEM without FBS at low density (not confluent) for 12 h and then stimulated with or without TGF β 1 (2 ng/ml) for another 2 h. Cells were lysed, and protein extracts were incubated overnight with antibodies and precipitated with protein A/G plus-agarose (Santa Cruz Biotechnology). Antibodies used in immunoprecipitation were: anti-YAP1 (Sigma, Y4770), anti-Smad2/3 (BD, 610842), anti-Smad4 (Santa Cruz Biotechnology, sc-7966), mouse IgG (JIR, 015-000-003), rabbit IgG (JIR, 011-000-004). Immunoprecipitates were resolved by 10% SDS-PAGE. Proteins were transferred onto PVDF (Millipore) using a Mini TransBlot system (Bio-Rad). The membranes were blocked with 5% milk in PBST and incubated overnight at 4 °C with antibodies, followed by incubation with HRP-conjugated secondary antibodies for 1 h at room temperature. Signals were detected by enhanced chemiluminescence (Pierce) according to the manufacturer's instructions. Antibodies used in Western blotting were: anti-YAP1 (Santa Cruz Biotechnology, sc-101199), anti-Smad2/3 (BD, 610842), anti-Smad4 (Santa Cruz Biotechnology, sc-7966), HRP-anti-rabbit IgG (JIR, 711-035-152), HRP-anti-mouse IgG (JIR, 115-035-174). For immunoprecipitation in E9.5 embryos, anti-YAP1 (Santa Cruz Biotechnology, sc-101199) was used and anti-YAP1 (Sigma, Y4770) was used in Western blotting. Other antibodies similar to HUVECs were used for immunoprecipitation

and Western blotting. ChIP-PCR or ChIP-qPCR assays were performed using the chromatin immunoprecipitation assay kit (Millipore, 17-295) following the protocol supplied by the manufacturer. Primers used are listed: Snail promoter –625/–502, sense (5'-TCGAATCCTCTGTTTATTCTGTCTGT-3') and antisense (5'-GGAGCCAGAAAGTGCGATGA-3'), Slug promoter –697/–576, sense (5'-GCCTGCCTTTAGAGGGCTA-C-3') and antisense (5'-TGCGCTACTCAGGGCTTC-3'), Gapdh, sense (5'-AGCTCAGGCCTCAAGACC-TT-3') and antisense (5'-AAGAAGATGCGGCTGACTGT-3').

Statistic Analysis—Data were analyzed by unpaired Student's *t*-tests for two groups, and ANOVA for over two groups test. Significance was accepted when $p < 0.05$. Results are shown as mean \pm S.E. values. For the counting of AV cushion mesenchymal cells, at least three embryos of each genotype were sectioned. At least three sections of each embryo were counted. For measuring distance in cell motility assay, 10 pictures of each group were collected, and 3 points of each picture were measured.

RESULTS

Loss of YAP1 in AV Endocardial Cushion Leads to Embryonic Lethality—We first inactivated a conditional YAP1 floxed allele (YAP1^{fl}) (22) in endothelial cells using Tie2-Cre (21) (Fig. 1A). To measure the extent of YAP1 inactivation, we performed *in situ* hybridization on Tie2-Cre; YAP1^{fl/+} (control) and Tie2-Cre; YAP1^{fl/fl} (mutant) embryos at E9.5, and found that *Yap1* mRNA was reduced in the endocardial cushions of mutant embryos (Fig. 1B). We also collected AV endocardial cushions and measured *Yap1* mRNA by quantitative RT-PCR. YAP1 expression was significantly reduced in mutant samples (Fig. 1C). We collected 31 litters of offspring from mating of female YAP1^{fl/fl} with male Tie2-Cre; YAP1^{fl/+}, and found only 1 mutant (Tie2-Cre; YAP1^{fl/fl}) out of 197 mice at weaning (Fig. 1D), well below the expected Mendelian frequency. These data show that endothelial inactivation of YAP1 severely impaired embryonic or early postnatal development.

We first evaluated mutant embryos at E9.5 and E10.5. At E9.5, mutant embryos appeared grossly normal and had normal cardiac contraction in all samples (Fig. 1E). However, at E10.5, the embryos were growth retarded, and some had increased pericardial fluid (Fig. 1F). Tie2-Cre recombines floxed alleles in vascular endothelial cells in addition to endocardial cells. To evaluate mutant embryos for a vascular defect that could delay embryonic development, we examined the yolk sac from E9.5 and E10.5 embryos. At E9.5, the vascular plexuses of mutant embryos and yolk sacs were grossly comparable to those of heterozygous littermates (Fig. 1, E, G, H), but at E10.5 yolk sac vascular remodeling and maturation were disrupted (Fig. 1F). Such yolk sac vascular abnormalities have been observed in mutant embryos with impaired heart function (27), so this defect might reflect a cell autonomous function of YAP1 in the extracardiac vasculature, or it might reflect impaired heart function. To avoid nonspecific abnormalities caused by global embryonic development delay, we focused on E9.5 embryos to study the role of YAP1 in cardiac cushion development.

YAP1 Function in Cardiac Valve Development

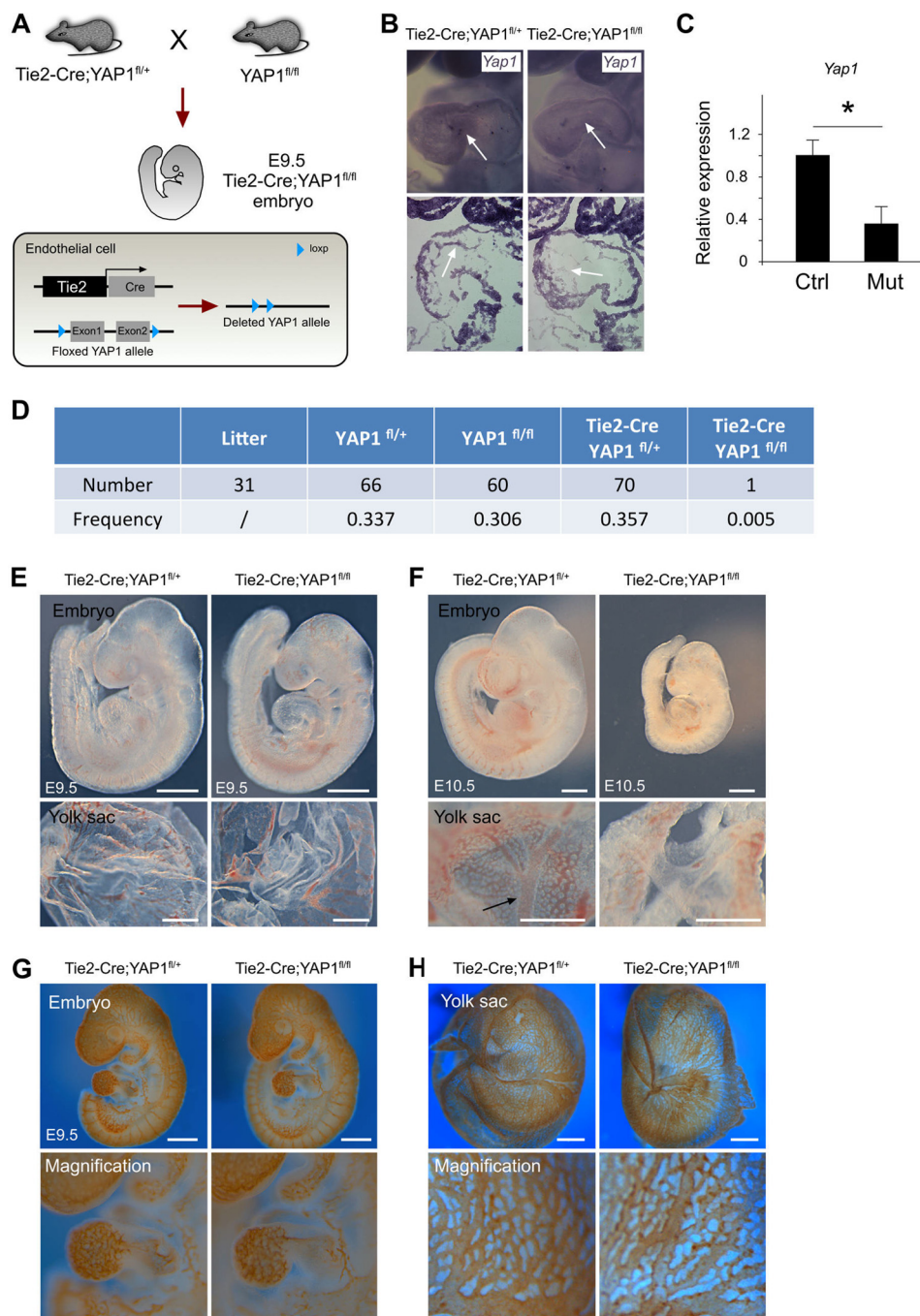


FIGURE 1. Endocardial specific deletion of YAP1 leads to embryonic death. *A*, schematic figure showing generation of YAP1 deletion in endocardial cells by Tie2-Cre. *B*, *in situ* hybridization of YAP1 shows reduced signal in endocardial cells (arrows) in Tie2-Cre;YAP1^{fl/fl} mutant. *C*, qRT-PCR of YAP1 from atrioventricular cushion. *, $p < 0.05$; $n = 9$. *D*, genotyping result of weaned litters. Frequency is calculated as the fraction of mice with indicated genotype to all mice. *E* and *F*, gross morphology of representative mutant and control embryos and yolk sacs at E9.5 and E10.5. Black arrow denotes remodeled vessels in control yolk sac. *G* and *H*, whole mount PECAM staining of E9.5 mutant and littermate control embryos and yolk sacs. White bar, 0.5 mm.

Inactivation of YAP1 in the Endocardium Impaired EMT of AV Cushion—To determine the effect of endocardial inactivation of YAP1 on heart development, we examined serial sections of E9.5 mutant and control hearts. In control hearts, AV cushions were populated by mesenchymal cells formed by endocardial EMT. However, very few mesenchymal cells were observed in the endocardial cushions of mutant embryos (Fig. 2*A*). Quantification of the cellularity of mutant and control cushions showed that the number of mesenchymal cells in both superior and inferior cushions was more than 10 times lower

than that of littermate controls (Fig. 2*B*). A similar conclusion was reached by scanning electron microscopy, which revealed significantly fewer mesenchymal cells in the mutant AV cushion region, compared with littermate control (Fig. 2*C*).

Because YAP1 is an important regulator of cell proliferation, we examined the effect of YAP1 inactivation on proliferation of endocardial cells. To determine if the defect in EMT results from a lack of proliferation, we measured endocardial cells positive for the proliferation marker phosphorylated histone H3 (pHH3). In the mutant, the fraction of proliferating endocardial

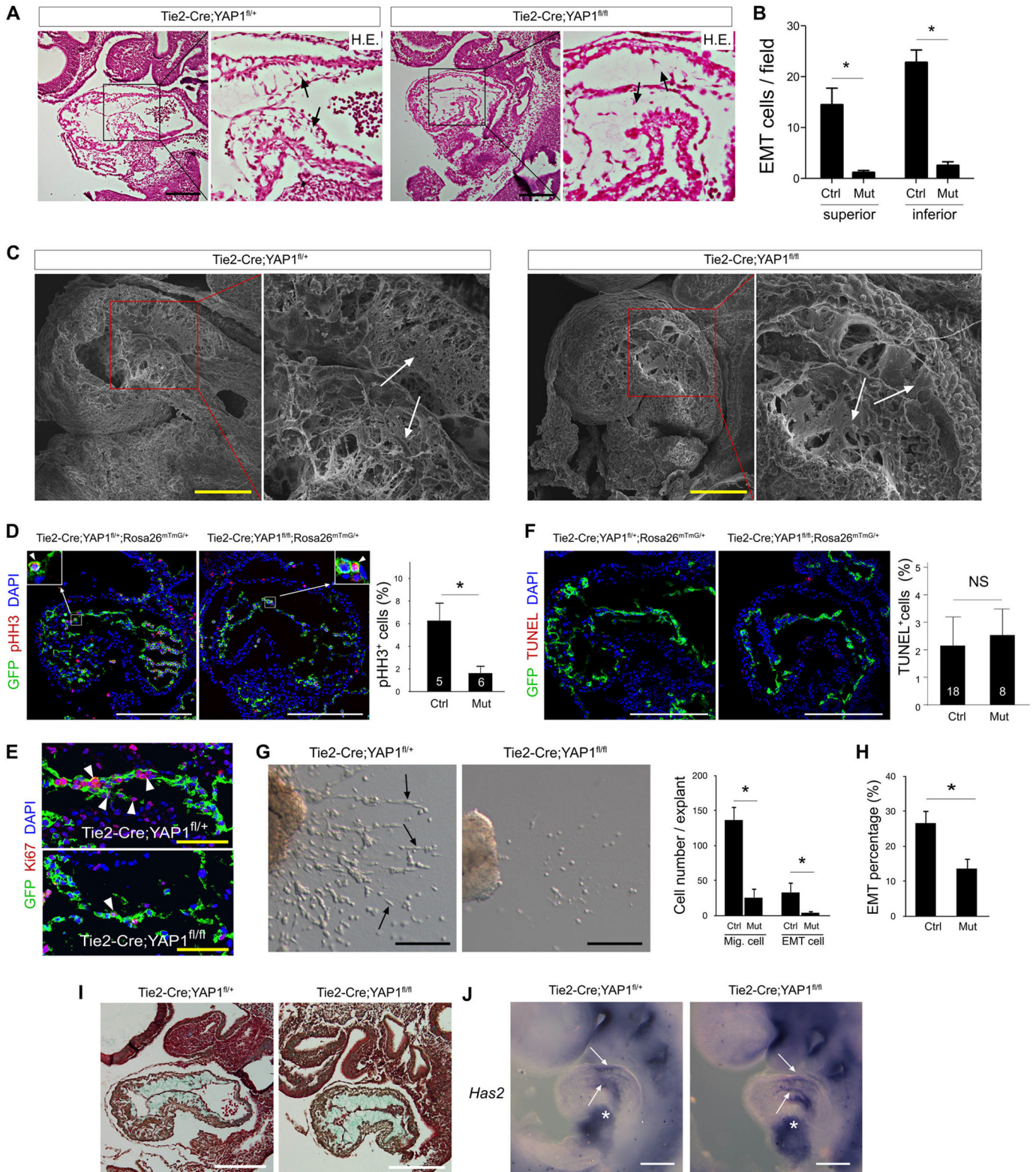


FIGURE 2. Endocardial cushion defect in YAP1 mutant embryos. A, H.E. staining of E9.5 embryonic sections. Black arrows indicate the superior and inferior AV cushion. B, quantification of mesenchymal cells in the superior and inferior AV cushion. *, *p* < 0.05; *n* = 4. C, scanning electron microscopic pictures of E9.5 control and mutant endocardial cushion. White arrows indicate the superior and inferior AV cushion. D, proliferation marker pHH3 staining of E9.5 mutant and littermate control embryos. *, *p* < 0.05; *n* = 5–6. E, Ki67 staining of E9.5 mutant and littermate controls. Arrowheads indicate Ki67 positive endocardial cells. F, TUNEL assay of cushion endocardial cell apoptosis in E9.5 mutant and control heart. NS, not significant. G, *in vitro* explant assay of E9.5 cushion, and quantification of migrating cells and spindle shaped cells (black arrows, EMT) from endocardial cushion. *, *p* < 0.05; *n* = 6 (mutant). H, quantification of spindle-shaped cells (EMT) among migrating cells. *, *p* < 0.05; *n* = 31 (control); *n* = 6 (mutant). I, Alcian blue staining shows no significant difference in extracellular matrix between control and mutant hearts. J, *in situ* hybridization showed that hyaluronan synthase-2 (*Has2*) expression was not significantly decreased in mutant AV cushion. Asterisk indicates proepicardium. White or black bar, 200 μ m; yellow bar, 100 μ m.

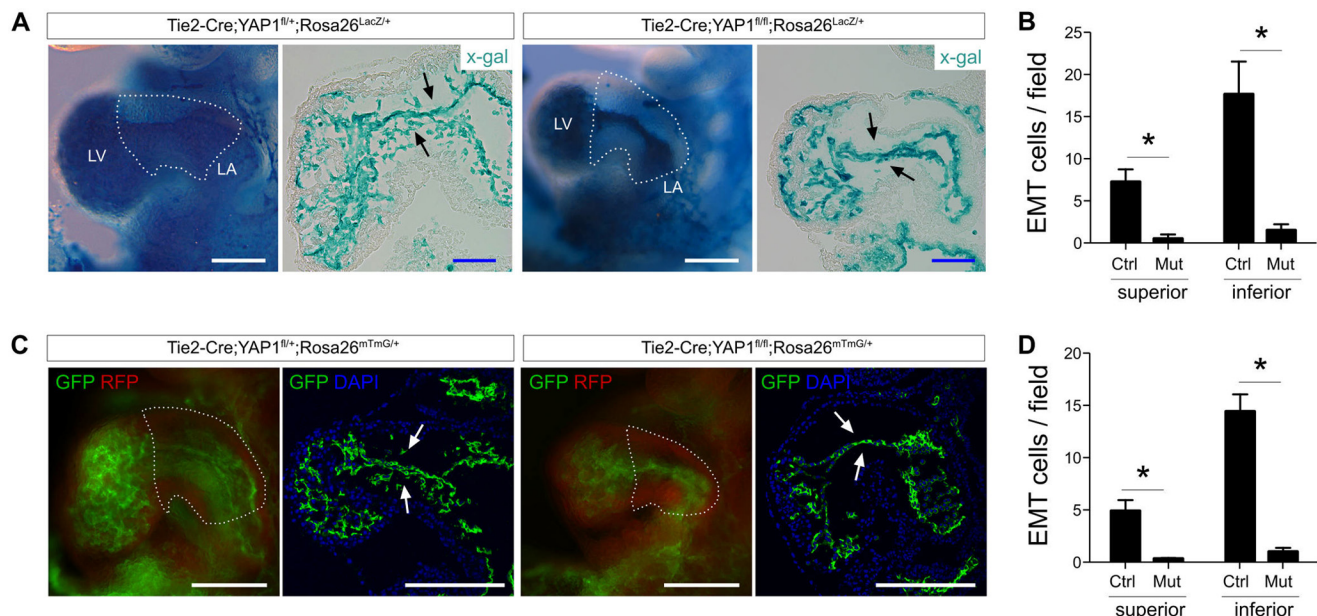


FIGURE 3. EMT defect in YAP1 mutants. *A*, genetic fate map of endocardium-derived cells by x-gal staining of Tie2-Cre;Rosa26^{LacZ/+} embryos. Mutant endocardial cushion showed reduced EMT compared with controls. *Black arrows* indicate endocardial cushions. *B*, quantification of x-gal-stained, endocardium-derived mesenchymal cells in the superior and inferior AV cushion. *, $p < 0.05$; $n = 3-5$. *C*, lineage tracing of endocardium-derived cells by Tie2-Cre;Rosa26^{mTmG/+} showed reduced EMT in mutant endocardial cushion compared with controls (*white arrows*). *D*, quantification of endocardium-derived cells in the superior and inferior AV cushion. *, $p < 0.05$; $n = 3$. *White bar*, 200 μm ; *blue bar*, 100 μm .

cells was roughly 3-fold reduced (Fig. 2*D*). We also performed Ki67 staining and found significantly reduced number of Ki67-positive endocardial cells in mutant cushions compared with control ones (Fig. 2*E*). Apoptosis analysis by TUNEL showed no significant difference of endocardial cell apoptosis between the mutants and littermate controls, suggesting cell death does not account for significantly reduced mesenchymal cells (Fig. 2*F*). These results suggested that endothelial ablation of YAP1 resulted in reduced endocardial cell proliferation, which likely contributes to the hypocellular cushion defect in mutants.

To further test whether YAP1 is required for endocardial EMT, we performed *ex vivo* collagen gel assays to study AV cushion EMT. In control explants, cells (136.8 ± 19.4 cells/explant) were readily detected migrating into the collagen gel after 72 h of *ex vivo* culture, while significantly fewer migrating cells (25.8 ± 13.0 cells/explant) were observed in mutant explants (Fig. 2*G*). Migrating cells in the AV explant assay represent those cells that have undergone activation and delamination from the epithelial sheet of the endocardium (11). A subset of cells acquire an elongated spindle shape, characteristic of mesenchymal cells formed by EMT, while the remaining cells retain a rounded morphology, representing cells that have undergone activation but not transformation (11). Mutant explants yielded fewer cells with an elongated spindle shape (Fig. 2*G*). Quantitative analysis confirmed a statistically significant decrease in the number (4.3 ± 2.4 cells/explant in mutant *versus* 33.3 ± 14.4 cells/explant in control; $p < 0.05$) and percentage of spindle-shaped mesenchymal cells among all migrating cells ($13.7\% \pm 2.9$ mutant *versus* $26.7\% \pm 3.7$ control; $p < 0.05$; Fig. 2*H*) in mutant explants. These data suggest that impaired EMT in combination with reduced proliferation may account for abnormal development of YAP1-deficient cushions.

Proper formation of extracellular matrix (ECM) is crucial for endocardial EMT (28). To examine ECM integrity, we stained mutant and control heart sections with Alcian blue, which visualizes glycosaminoglycans that are major components of endocardial cushions. Alcian blue staining showed no significant difference between mutant and control cushions (Fig. 2*I*), suggesting that inactivation of YAP1 in endocardium did not affect ECM formation. In agreement with the Alcian blue staining, expression of hyaluronic acid (HA) synthase 2 (*Has2*), the gene responsible for deposition of the major glycosaminoglycan of the endocardial cushions, was not significantly changed in the AV cushions of mutants compared with control embryos (Fig. 2*J*).

Lineage Tracing Reveals Reduced EMT in Mutants—To provide genetic lineage tracing evidence of the endocardial EMT defect, we generated mutant embryos containing either the Rosa26^{LacZ} (24) or Rosa26^{mTmG} (23) Cre-reporter allele to allow visualization of endocardial cells and their derivatives in the AV cushions. Tie2-Cre efficiently inactivated target genes in endothelium and its derivatives, including in AV cushion mesenchymal cells (21). Whole mount and section X-gal staining of E9.5 control embryos showed mesenchymal cells in the AV cushion were Cre-labeled, indicating their origin from endothelial cells by EMT (Fig. 3*A*). While mutant endocardium of the AV cushions was efficiently Cre labeled ($\beta\text{-gal}^+$), labeled cells were rarely detected in the AV cushion of mutant embryos (Fig. 3*A*). Quantitative analysis showed that the number of $\beta\text{-gal}^+$ mesenchymal cells formed in both the inferior and superior AV cushions of mutant embryos was significantly lower than that of controls (Fig. 3*B*). Lineage tracing of endocardium-derived cells using the Rosa26^{mTmG} reporter showed consistent results, with reduced endocardium-derived mesenchymal cells in mutant cushions at E9.5 (Fig. 3, *C* and *D*). Collectively, these

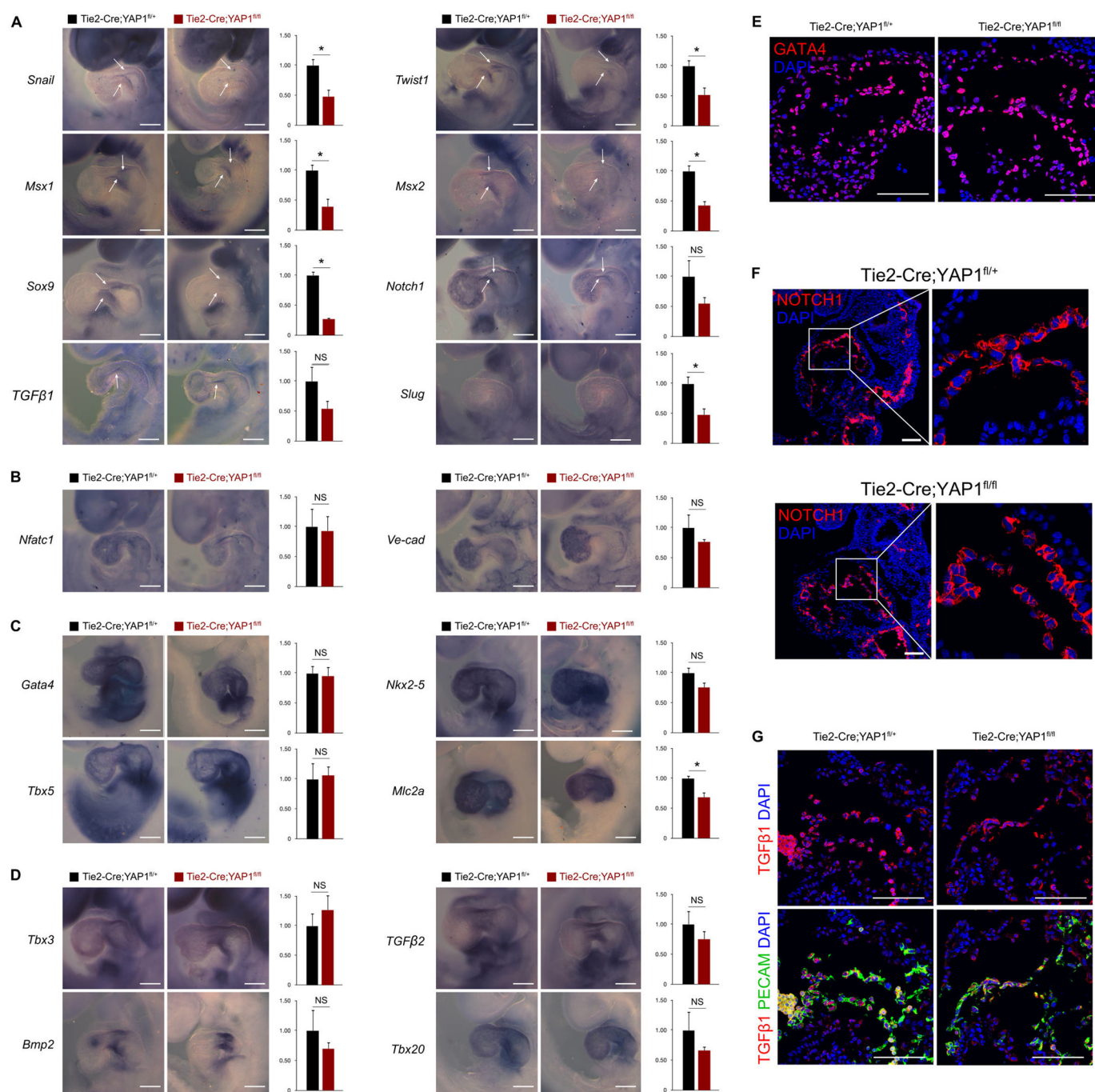


FIGURE 4. Loss of YAP1 leads to reduced expression of endocardial EMT markers. A, endocardial EMT markers *Snail*, *Twist1*, *Msx1*, *Msx2*, *Sox9*, and *Slug* were reduced in mutant (Tie2-Cre;YAP1^{fl/fl}) compared with littermate control (Tie2-Cre;YAP1^{fl/+}) endocardial cushions by *in situ* hybridization and qRT-PCR. *TGFβ1* and *Notch1* expression were not significantly reduced in mutants. B, endocardial markers *Nfatc1* and *Ve-cad* were normally expressed in mutants. C, cardiac differentiation markers *Gata4*, *Nkx2-5*, and *Tbx5* were normally expressed in mutants. *Mlc2a* was reduced in mutants. D, atrioventricular canal myocardium markers *Tbx3*, *Bmp2*, *TGFβ2*, and *Tbx20* were not significantly changed in mutants compared with littermate controls. White arrows indicate endocardial cushion. White bar, 200 μ m. Each *in situ* hybridization is representative of 2–4 replicates each genotype. *, $p < 0.05$, $n = 3$ –5 for qRT-PCR. NS, not significant. E, F, and G, immunostaining showed that GATA4, NOTCH1, and TGFβ1 expression were normal in endocardial cells of mutants compared with littermate controls. White bar, 100 μ m.

data indicate that inactivation of YAP1 in endocardium impairs AV valve development by interfering with endocardial EMT.

Endocardial Deletion of YAP1 Leads to Reduced Expression of EMT Genes—To understand the molecular mechanisms that explain the loss of EMT in YAP1 mutants, we performed *in situ* hybridization and quantitative RT-PCR to detect gene expression related to AV cushion development. The Snail family

members *Snail* (also known as *Snai1*) and *Slug* (also known as *Snai2*) encode zinc finger-containing transcriptional repressors that trigger EMT during embryonic development and tumor progression by regulating expression of junction protein *E-cadherin* (29). In the mouse, *Snail* is expressed in the AV cushion endocardium at the onset of EMT and is necessary for endocardial EMT (30). Likewise, *Slug* is required for initiation

YAP1 Function in Cardiac Valve Development

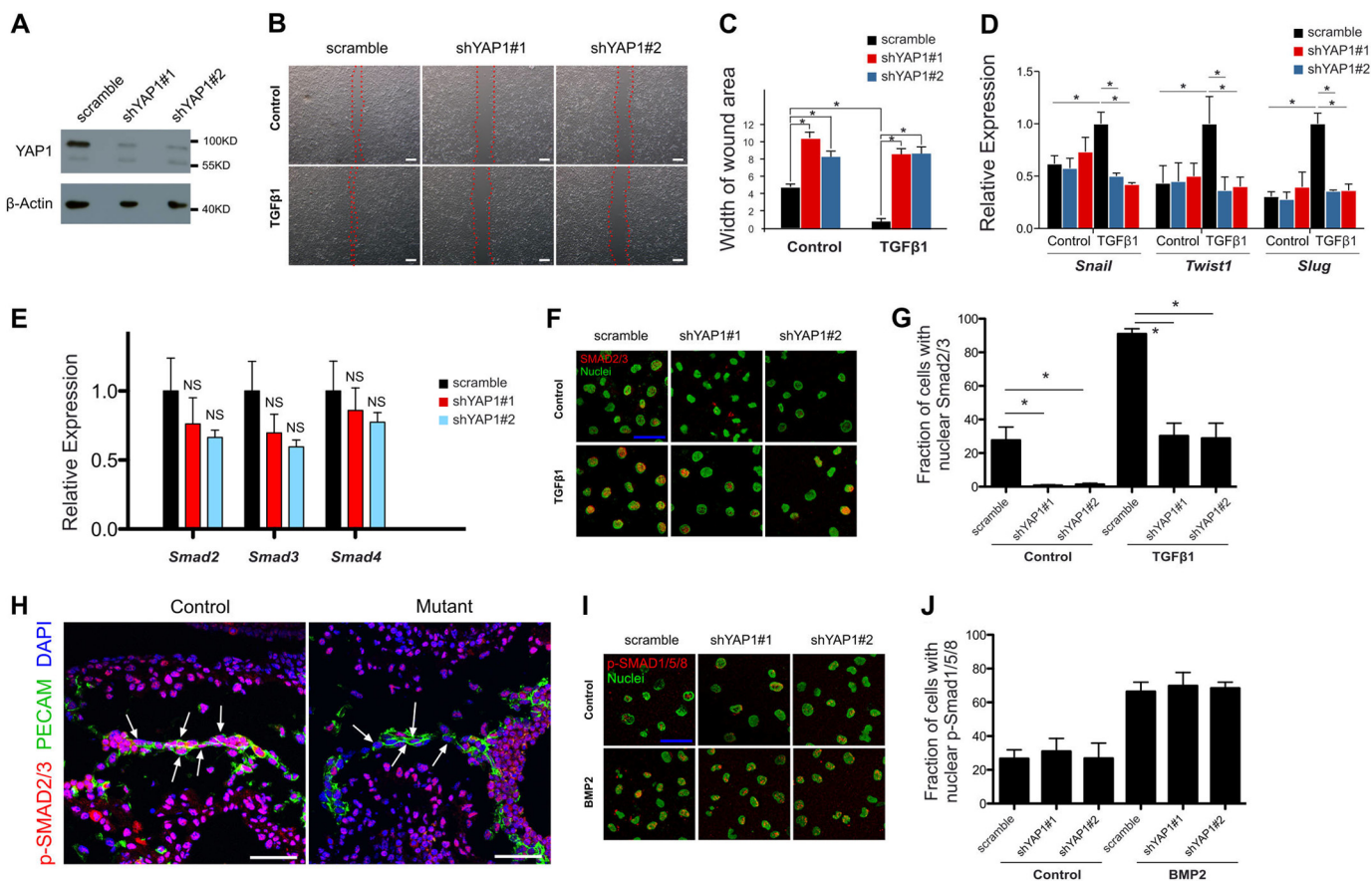


FIGURE 5. YAP1 regulates cell migration *in vitro* and mediates Smad2/3/4 nuclear entry. A, Western blot of YAP1 in HUVECs treated with YAP1 shRNA or scrambled shRNA. B, representative images of HUVEC cell motility assay. HUVECs treated with YAP1 or scramble shRNA were cultured in DMEM without FBS and with or without TGF β 1 stimulation (2 ng/ml) for 12 h. Bar, 0.2 mm. C, aggregate data for the width of wound area shown in B. *, $p < 0.05$; $n = 10$. D and E, after cell motility assay, relative expression of EMT marker genes (D) or *Smad2/3/4* (E) in YAP1-knock-down or scramble HUVECs treated with or without TGF β 1 was determined by qRT-PCR. *, $p < 0.05$; NS, not significant. $n = 4$. F, immunostaining of SMAD2/3 in YAP1-knock-down or scramble HUVECs, cultured at low density and treated with or without TGF β 1 (2 ng/ml) for 2 h. Bar, 50 μ m. G, quantification of nuclear SMAD2/3 positive cells among DAPI-positive cells. *, $p < 0.05$; $n = 6$. H, phosphorylated SMAD2/3 (p-SMAD2/3) staining on E9.5 embryonic cushion tissues showed less nuclear accumulation of p-Smad2/3 in mutant endocardium cells compared with controls. Arrows indicate endothelial cells. White bar, 50 μ m. I, immunostaining of p-SMAD1/5/8 in YAP1-knock-down or scramble HUVEC cells (cultured at low density) treated with or without BMP2 (50 ng/ml) for 2 h. Bar, 50 μ m. J, quantification of nuclear p-Smad1/5/8-positive cells among DAPI-positive cells. $n = 6$.

steps of EMT in chicken heart development (31). Loss of YAP1 in AV cushion endocardium reduced *Snail* expression, as measured by both *in situ* hybridization and qRT-PCR (Fig. 4A). *Slug* expression was also reduced in YAP1 mutant cushions by qRT-PCR (Fig. 4A). However, *Slug in situ* hybridization was not informative as we were unable to detect its expression in AV cushions at E9.5 (Fig. 4A). *Notch1*, which regulates *Snail* and *Slug* to promote AV cushion EMT (30, 32), was not significantly reduced in the mutant embryos compared with the controls (Fig. 4, A and F), suggesting that YAP1 regulates *Snail* and *Slug* expression independent of Notch1.

Next, we examined the transcription factors *Twist1*, *Sox9*, *Msx1*, and *Msx2*, which are expressed in the AV cushion mesenchyme and crucial for the proliferation and migration of these cells (33–35). We found that these EMT-related genes were significantly reduced in the YAP1 mutants (Fig. 4A). TGF β 1, which is a ligand for the TGF β signaling pathway and required for normal AV cushion development (36), was not significantly altered in YAP1 mutants (Fig. 4, A and G).

We next asked if YAP1-deficient endocardial cells maintained their molecular signature. Expression of the endocardial markers *Nfatc1* and *Ve-cadherin* were maintained in YAP1

mutant endocardium, suggesting that early AV endocardium specification was unaffected in the mutant embryos (Fig. 4B). Furthermore, expression of *Gata4*, *Tbx5*, and *Nkx2-5*, transcription factors required for growth and maturation of the fetal hearts and for endocardial cushion development (37–39) were also not significantly changed by endocardial YAP1 inactivation (Fig. 4C). GATA4 protein expression was neither significantly changed in mutants (Fig. 4E).

To determine whether deletion of *YAP1* in the endocardium might influence myocardial signals required for EMT, we used *in situ* hybridization and qRT-PCR to measure the expression of *Tbx3*, *TGF β 2*, *Bmp2*, and *Tbx20*, a set of important factors that are expressed in AV cushion myocardium. Expression of these factors was grossly normal in the AV cushions of mutant embryos (Fig. 4D), suggesting that AV myocardial development and signaling were relatively unperturbed by endothelial YAP1 knock-out.

YAP1 Cooperates with TGF β /Smad Signaling Pathway to Regulate *Snail*, *Slug*, and *Twist1* Expression in Endothelial Cells—In an attempt to identify the specific mechanisms that relate YAP1 and EMT, we knocked down *YAP1* with two shRNAs (shYAP1#1 and shYAP1#2). The lentiviruses expressing these

shRNAs significantly inhibited YAP1 expression in human umbilical vein endothelial cells (HUVECs) (Fig. 5A). As migration is an important initial step in EMT, we then tested cell motility using a wound healing assay to analyze the cellular function of YAP1 on EMT *in vitro*. At 12 h after wounding, YAP1 knock-down cells showed markedly reduced motility (Fig. 5B). Addition of TGF β 1 enhanced migration of endothelial cells (Fig. 5B) and this pro-migratory effect was significantly blocked by YAP1 knock-down (Fig. 5B and 5C). *Snail*, *Slug*, and *Twist1* are all downstream targets of TGF β signaling, and are regulated by Smad2/3/4 complex (40–43). Next we harvested the endothelial cells used in the wound healing assay and measured the expression level of *Snail*, *Slug*, and *Twist1* by qRT-PCR. Expression of these transcription factors, which were induced by TGF β 1 stimulation, was significantly down-regulated in YAP1 knock-down endothelial cells (Fig. 5D). However, YAP1-knock-down did not significantly alter the expression of *Smad2*, *Smad3*, or *Smad4* (Fig. 5E), indicating that reduced *Snail*, *Slug*, and *Twist1* expression after YAP1 knock-down are not caused by down-regulation of Smad2/3/4.

To determine whether TGF β -induced Smad nuclear localization was altered by YAP1 knock-down, we performed SMAD2/3 immunostaining in endothelial cells cultured at low density (not confluent). Without TGF β 1 treatment, 27.6% cells treated with scrambled shRNA were nuclear Smad2/3 positive (Fig. 5, F and G). In YAP1-knock-down, 0.7%–1.3% cells were nuclear SMAD2/3 positive (Fig. 5, F and G). After treatment with TGF β 1 for 2 h, SMAD2/3 accumulated in the nucleus. Over 90% of control cells were nuclear SMAD2/3 positive (Fig. 5, F and G). However, fewer YAP1-knock-down cells (~30%) were nuclear Smad2/3 positive. We also performed p-SMAD2/3 staining on E9.5 embryonic cushions and found less nuclear accumulation of p-SMAD2/3 in mutant endocardial cells compared with control ones (Fig. 5H). These *in vitro* and *in vivo* data suggest YAP1 regulates SMAD2/3 accumulation in the nucleus.

Recent studies indicate that *Twist1* and *Snail* expression and endocardial EMT are also regulated by BMP2 (44, 45). On the molecular level, the BMP signaling pathway functions through phosphorylation and nuclear localization of the SMAD1/5/8 complex. Therefore we also performed immunostaining to detect p-SMAD1/5/8 in endothelial cells and found that YAP1 knockdown did not significantly affect p-SMAD1/5/8 expression or nuclear localization (Fig. 5, I and J).

YAP1 is a transcriptional co-activator. We hypothesized that it might modulate TGF β signaling by interacting with the SMAD2/3/4 transcriptional complex. To directly test this hypothesis, we performed co-immunoprecipitation assay from HUVECs and from E9.5 embryos. This demonstrated an interaction between YAP1 and SMAD2/3/4 complex both in HUVECs, which were treated with TGF β 1, and E9.5 embryos (Fig. 6, A and B). The SMAD2/3/4 complex was shown previously to regulate *Snail* and *Slug* expression directly by binding to their promoters (42, 43). We asked if YAP1 also bound to the same sites through binding to SMAD2/3/4 complex. By ChIP-PCR and ChIP-qPCR assays, we found YAP1 binds the same *Snail* and *Slug* proximal promoter in response to TGF β 1 treatment (Fig. 6C). We next tested whether YAP1 affects the transcriptional activity of SMAD2/3/4 using a luciferase reporter

that was driven by four repeats of SMAD binding elements (SBE), described previously (46). As expected, overexpression of the constitutively active TGF β type I receptor (ca-Alk5) or treatment with TGF β 1 (2 ng/ml) for 16 h stimulated the luciferase reporter (Fig. 6D). However, luciferase activity decreased significantly in YAP1-knock-down cells, with or without overexpression of ca-Alk5 or TGF β 1 treatment (Fig. 6D). These data suggested that YAP1-Smad2/3/4 interaction promoted Smad transcriptional activity and potentiated TGF β signaling.

Taken together, our work shows that YAP1 regulates AV cushion development by regulating endocardial proliferation and EMT. YAP1 may influence EMT by enhancing Smad transcriptional outputs downstream of TGF β 1. In the absence of YAP1, TGF β 1 signaling is down-regulated, leading to decreased expression of EMT genes *Snail*, *Twist1*, and *Slug*.

DISCUSSION

The importance of Hippo signaling to YAP1 in the regulation of organ size and cellular proliferation is now well recognized. However, less is known about how this pathway controls cell state transitions that are critical for development and oncogenesis. In this study, we show that YAP1 is an essential regulator of AV cushion EMT, a well studied developmental cell state transition that is essential for heart valve formation. We provide mechanistic insight into YAP1 control of EMT by showing that YAP1 potentiates TGF β -driven Smad signaling to regulate expression of the downstream target genes *Snail*, *Slug*, and *Twist1*, the important transcriptional regulators of EMT.

Endocardial ablation of YAP1 resulted in markedly hypoplastic endocardial cushions. In part, this was due to reduced proliferation of endocardial cells, consistent with YAP1's established mitogenic activity. We also found that YAP1 regulates endocardial EMT, thus adding a new mechanism that governs cushion development. YAP1 was previously implicated in promoting tumor metastasis, a process related to EMT (20). However, whether YAP1 promotes EMT during oncogenic transformation *in vivo*, in addition to tumor growth, is not known. Our study shows that YAP1 is required during development to promote EMT in the endocardial cushions and suggests that it may similarly promote EMT in other developmental contexts or in oncogenesis, as these different forms of EMT share some common molecular regulation. Further studies are required to determine whether YAP1 is deployed to regulate EMT in other developmental or oncogenic contexts.

YAP1 may regulate endocardial EMT through multiple mechanisms. Our studies delineate one mechanism, in which YAP1 is required for TGF β signaling by interacting with the Smad2/3/4 complex. Interestingly, a recent study (47) also linked Hippo signaling pathway with TGF β signaling by showing that TGF β stimulates Smad2/3/4 binding to WWTR1 (also known as TAZ), a YAP1 paralogue. As a result, WWTR1 was recruited to TGF β response elements in human embryonic stem cells (47). Loss of *WWTR1* led to failure of Smad2/3/4 complexes to accumulate in the nucleus and activate transcription (47). Whether Hippo signaling pathway potentiates or inhibits TGF β signaling is also highly context dependent. In high-density Eph4 epithelial cell cultures, the Hippo kinase activation promoted cytoplasmic localization of YAP1/WWTR1,

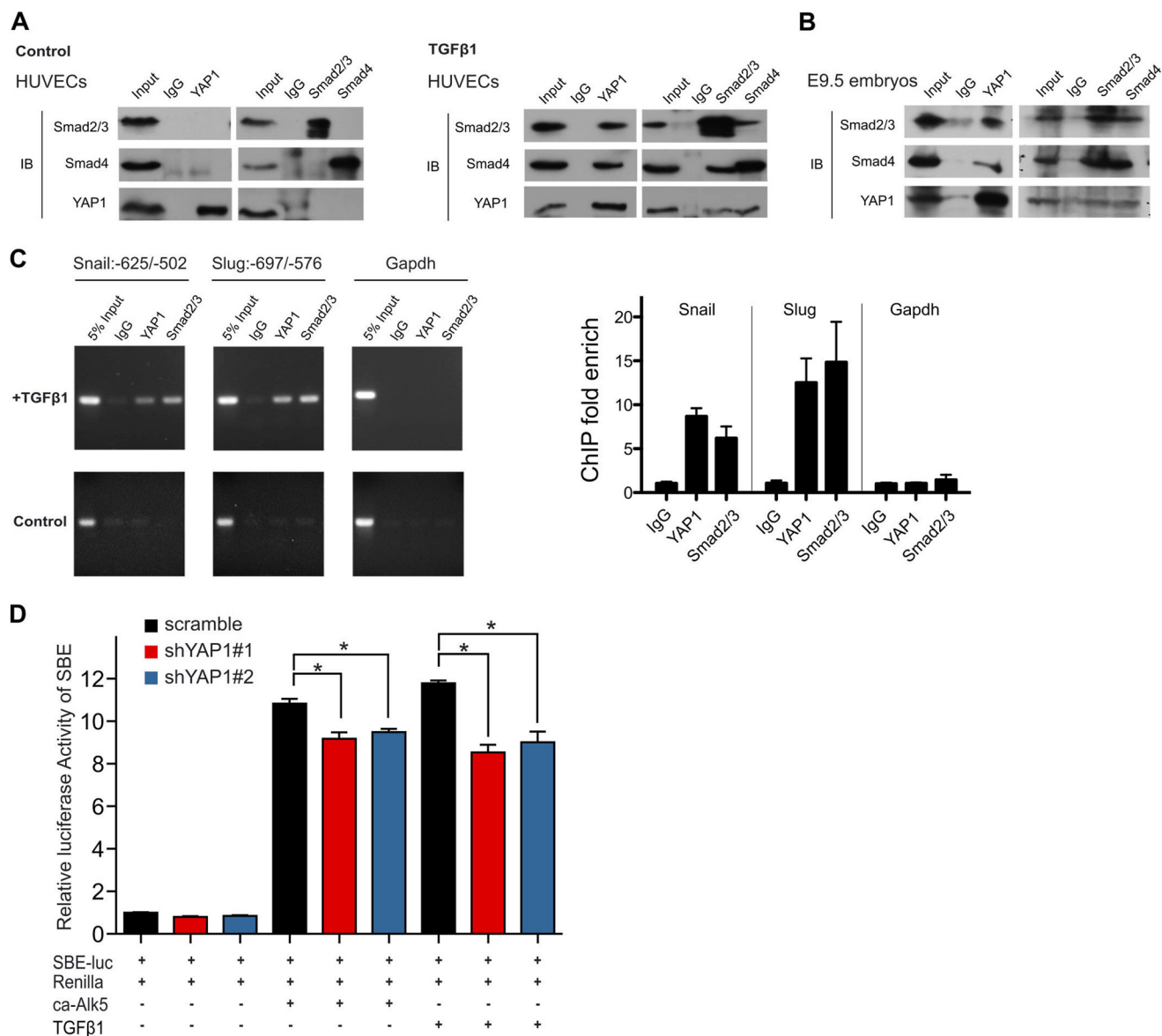


FIGURE 6. YAP1 interacts with Smad2/3/4 to regulate EMT genes. *A*, *in vitro* Co-IP experiments in HUVECs cultured at low density in DMEM without FBS for 12 h and then treated with or without TGFβ1 (2 ng/ml) for 2 h. Lysates were immunoprecipitated using anti-YAP1 (Sigma, Y4770), anti-SMAD2/3 (BD, 610842), or anti-SMAD4 (Santa Cruz Biotechnology, sc-7966) antibodies, respectively. The immunoprecipitates were probed using anti-YAP1 (Santa Cruz Biotechnology, sc-101199), anti-SMAD2/3 (BD, 610842), or anti-SMAD4 antibodies (Santa Cruz Biotechnology, sc-7966). *B*, *in vivo* Co-IP experiments in E9.5 embryos. *C*, ChIP-PCR and ChIP-qPCR experiments were performed in HUVECs to test enrichment of *Snail* –625/–502 and *Slug* –697/–576, promoter region sequences in ChIP DNA obtained with anti-YAP1 (Sigma, Y4770) or anti-SMAD2/3 (BD, 610842). *Gapdh* was a negative control. HUVECs were cultured at low density in DMEM without FBS for 12 h and then treated with or without TGFβ1 (2 ng/ml) for 2 h. *D*, luciferase activity comparison of SBE in YAP1-knock-down or scramble 293T cells transfected with ca-Alk5 or treated with TGFβ1 (2 ng/ml) for 16 h. *, $p < 0.05$.

which sequestered Smad2/3/4 complexes and suppressed TGFβ signaling (48). However, knockdown of either WWTR1 or YAP1 did not affect Smad2/3 nuclear accumulation, whereas knockdown of both prevented Smad2/3 nuclear accumulation (48). Further studies are needed to understand the factors that determine whether WWTR1 or YAP1 can effectively partner with Smads to potentiate TGFβ signaling.

YAP1 is a transcriptional coactivator that does not bind DNA directly, but rather interacts with DNA-binding transcription factors to stimulate gene expression. The TEAD family of transcription factors has been most closely related to YAP1, although several other transcription factors have been implicated as YAP1 partners, including the p53-related p73, RUNX2,

the ErbB4 cytoplasmic domain, and Tbx5 (49–53). Thus we suspected TEAD might also play an important role in regulating endocardial EMT through formation of a YAP1/TEAD/Smad complex. However, we did not find any TEAD binding site in a 10-kb region upstream of *Snail*, *Slug*, or *Twist1* promoters, including the sites adjacent to Smad binding sites (data not shown). This suggests that YAP1 may regulate endocardial EMT independently of the canonical YAP1/TEAD complex.

Our finding that YAP1-Smad2/3/4 transcriptional regulation is essential for endocardial EMT is consistent with a previous study of endocardial inactivation of Smad4 (54). Like YAP1 endocardial loss of function, Smad4 endocardial knock-out

caused hypocellular endocardial cushions at E9.5, reduced proliferation and survival of cushion mesenchymal cells, and impaired endocardial EMT. These data further suggest requirement of YAP1/Smad complex for AV cushion development.

In our study, we used Tie2-Cre to inactivate a conditional YAP1 allele. This Cre driver labels both endocardial cells and vascular endothelial cells. While YAP1 may regulate vascular development, the effects that we observed on heart valve development are likely to be primary since we did not detect a significant vascular phenotype in mutant embryos or yolk sacs at E9.5, the time point at which we studied the valve development phenotype. Furthermore, the *ex vivo* AV explant studies further demonstrated that the defect was intrinsic to the AV cushions and not the embryonic environment. Therefore, our study clearly demonstrates that YAP1 is required in AV cushion endocardium for normal endocardial cushion development.

In conclusion, we demonstrate that YAP1 plays a critical role during AV cushion development, regulating formation of valve mesenchymal progenitor cells by endocardial EMT. YAP1 potentiated TGF β 1 signaling by controlling Smad2/3/4 nuclear accumulation and regulating downstream targets *Snail*, *Slug*, and *Twist1* expression. Information acquired from this study will help us to better understand mechanisms of congenital heart diseases involving AV valve abnormalities, and may also have ramifications for understanding EMT in the development of other organ systems and in cancer.

Acknowledgments—We thank Yan Chen and Bin Zhao for providing plasmids.

REFERENCES

- Onuzo, O. C. (2006) How effectively can clinical examination pick up congenital heart disease at birth? *Archives of disease in childhood. Fetal and neonatal edition* **91**, F236–F237
- Barnett, J. V., and Desgrosellier, J. S. (2003) Early events in valvulogenesis: a signaling perspective. *Birth Defects Research* **69**, 58–72
- Hoffman, J. I., and Kaplan, S. (2002) The incidence of congenital heart disease. *J. Am. College Cardiol.* **39**, 1890–1900
- Markwald, R. R., Krook, J. M., Kitten, G. T., and Runyan, R. B. (1981) Endocardial cushion tissue development: structural analyses on the attachment of extracellular matrix to migrating mesenchymal cell surfaces. *Scanning Electron Microscopy* 261–274
- Eisenberg, L. M., and Markwald, R. R. (1995) Molecular regulation of atrioventricular valvuloseptal morphogenesis. *Circ. Res.* **77**, 1–6
- von Gise, A., and Pu, W. T. (2012) Endocardial and epicardial epithelial to mesenchymal transitions in heart development and disease. *Circ. Res.* **110**, 1628–1645
- Peinado, H., Olmeda, D., and Cano, A. (2007) Snail, Zeb and bHLH factors in tumour progression: an alliance against the epithelial phenotype? *Nat. Rev. Cancer* **7**, 415–428
- Brown, C. B., Boyer, A. S., Runyan, R. B., and Barnett, J. V. (1996) Antibodies to the Type II TGF β receptor block cell activation and migration during atrioventricular cushion transformation in the heart. *Dev. Biol.* **174**, 248–257
- Brown, C. B., Boyer, A. S., Runyan, R. B., and Barnett, J. V. (1999) Requirement of type III TGF- β receptor for endocardial cell transformation in the heart. *Science* **283**, 2080–2082
- Boyer, A. S., Ayerinskas II, Vincent, E. B., McKinney, L. A., Weeks, D. L., and Runyan, R. B. (1999) TGF β 2 and TGF β 3 have separate and sequential activities during epithelial-mesenchymal cell transformation in the embryonic heart. *Dev. Biol.* **208**, 530–545
- Camenisch, T. D., Molin, D. G., Person, A., Runyan, R. B., Gittenberger-de Groot, A. C., McDonald, J. A., and Klewer, S. E. (2002) Temporal and distinct TGF β ligand requirements during mouse and avian endocardial cushion morphogenesis. *Dev. Biol.* **248**, 170–181
- Heallen, T., Zhang, M., Wang, J., Bonilla-Claudio, M., Klysik, E., Johnson, R. L., and Martin, J. F. (2011) Hippo pathway inhibits Wnt signaling to restrain cardiomyocyte proliferation and heart size. *Science* **332**, 458–461
- Xin, M., Kim, Y., Sutherland, L. B., Qi, X., McAnally, J., Schwartz, R. J., Richardson, J. A., Bassel-Duby, R., and Olson, E. N. (2011) Regulation of insulin-like growth factor signaling by Yap governs cardiomyocyte proliferation and embryonic heart size. *Science Signal.* **4**, ra70
- Xin, M., Kim, Y., Sutherland, L. B., Murakami, M., Qi, X., McAnally, J., Porrello, E. R., Mahmoud, A. I., Tan, W., Shelton, J. M., Richardson, J. A., Sadek, H. A., Bassel-Duby, R., and Olson, E. N. (2013) Hippo pathway effector Yap promotes cardiac regeneration. *Proc. Natl. Acad. Sci. U.S.A.* **110**, 13839–13844
- von Gise, A., Lin, Z., Schlegelmilch, K., Honor, L. B., Pan, G. M., Buck, J. N., Ma, Q., Ishiwata, T., Zhou, B., Camargo, F. D., and Pu, W. T. (2012) YAP1, the nuclear target of Hippo signaling, stimulates heart growth through cardiomyocyte proliferation but not hypertrophy. *Proc. Natl. Acad. Sci. U.S.A.* **109**, 2394–2399
- Hao, Y., Chun, A., Cheung, K., Rashidi, B., and Yang, X. (2008) Tumor suppressor LATS1 is a negative regulator of oncogene YAP. *J. Biol. Chem.* **283**, 5496–5509
- Overholtzer, M., Zhang, J., Smolen, G. A., Muir, B., Li, W., Sgroi, D. C., Deng, C. X., Brugge, J. S., and Haber, D. A. (2006) Transforming properties of YAP, a candidate oncogene on the chromosome 11q22 amplicon. *Proc. Natl. Acad. Sci. U.S.A.* **103**, 12405–12410
- Vitolo, M. I., Anglin, I. E., Mahoney, W. M., Jr., Renoud, K. J., Gartenhaus, R. B., Bachman, K. E., and Passaniti, A. (2007) The RUNX2 transcription factor cooperates with the YES-associated protein, YAP65, to promote cell transformation. *Cancer Biol. Ther.* **6**, 856–863
- Zhang, X., Milton, C. C., Humbert, P. O., and Harvey, K. F. (2009) Transcriptional output of the Salvador/warts/hippo pathway is controlled in distinct fashions in *Drosophila melanogaster* and mammalian cell lines. *Cancer Res.* **69**, 6033–6041
- Lamar, J. M., Stern, P., Liu, H., Schindler, J. W., Jiang, Z. G., and Hynes, R. O. (2012) The Hippo pathway target, YAP, promotes metastasis through its TEAD-interaction domain. *Proc. Natl. Acad. Sci. U.S.A.* **109**, E2441–E2450
- Kisanuki, Y. Y., Hammer, R. E., Miyazaki, J., Williams, S. C., Richardson, J. A., and Yanagisawa, M. (2001) Tie2-Cre transgenic mice: a new model for endothelial cell-lineage analysis *in vivo*. *Dev. Biol.* **230**, 230–242
- Schlegelmilch, K., Mohseni, M., Kirak, O., Pruszk, J., Rodriguez, J. R., Zhou, D., Kreger, B. T., Vasioukhin, V., Avruch, J., Brummelkamp, T. R., and Camargo, F. D. (2011) Yap1 acts downstream of α -catenin to control epidermal proliferation. *Cell* **144**, 782–795
- Muzumdar, M. D., Tasic, B., Miyamichi, K., Li, L., and Luo, L. (2007) A global double-fluorescent Cre reporter mouse. *Genesis* **45**, 593–605
- Soriano, P. (1999) Generalized lacZ expression with the ROSA26 Cre reporter strain. *Nat. Genet.* **21**, 70–71
- Wilkinson, D. G. (1992) *In Situ Hybridization: A Practical Approach*, Oxford University Press, New York
- Zhou, B., Ma, Q., Kong, S. W., Hu, Y., Campbell, P. H., McGowan, F. X., Ackerman, K. G., Wu, B., Zhou, B., Tevosian, S. G., and Pu, W. T. (2009) Fog2 is critical for cardiac function and maintenance of coronary vasculature in the adult mouse heart. *J. Clin. Invest.* **119**, 1462–1476
- Tanaka, M., Chen, Z., Bartunkova, S., Yamasaki, N., and Izumo, S. (1999) The cardiac homeobox gene *Csx/Nkx2.5* lies genetically upstream of multiple genes essential for heart development. *Development* **126**, 1269–1280
- Camenisch, T. D., Spicer, A. P., Brehm-Gibson, T., Biesterfeldt, J., Augustine, M. L., Calabro, A., Jr., Kubalak, S., Klewer, S. E., and McDonald, J. A. (2000) Disruption of hyaluronan synthase-2 abrogates normal cardiac morphogenesis and hyaluronan-mediated transformation of epithelium to mesenchyme. *J. Clin. Invest.* **106**, 349–360
- Nieto, M. A. (2002) The snail superfamily of zinc-finger transcription factors. *Nature Reviews. Mol. Cell Biol.* **3**, 155–166
- Timmerman, L. A., Grego-Bessa, J., Raya, A., Bertran, E., Pérez-Pomares, J. M., Díez, J., Aranda, S., Palomo, S., McCormick, F., Izpisua-Belmonte, J. C., and de la Pompa, J. L. (2004) Notch promotes epithelial-mesenchymal

- mal transition during cardiac development and oncogenic transformation. *Genes Dev.* **18**, 99–115
31. Romano, L. A., and Runyan, R. B. (2000) Slug is an essential target of TGF β 2 signaling in the developing chicken heart. *Dev. Biol.* **223**, 91–102
32. Niessen, K., Fu, Y., Chang, L., Hoodless, P. A., McFadden, D., and Karsan, A. (2008) Slug is a direct Notch target required for initiation of cardiac cushion cellularization. *J. Cell Biol.* **182**, 315–325
33. Shelton, E. L., and Yutzey, K. E. (2008) Twist1 function in endocardial cushion cell proliferation, migration, and differentiation during heart valve development. *Dev. Biol.* **317**, 282–295
34. Akiyama, H., Chaboissier, M. C., Behringer, R. R., Rowitch, D. H., Schedl, A., Epstein, J. A., and de Crombrughe, B. (2004) Essential role of Sox9 in the pathway that controls formation of cardiac valves and septa. *Proc. Natl. Acad. Sci. U.S.A.* **101**, 6502–6507
35. Boogerd, K. J., Wong, L. Y., Christoffels, V. M., Klarenbeek, M., Ruijter, J. M., Moorman, A. F., and Barnett, P. (2008) Msx1 and Msx2 are functional interacting partners of T-box factors in the regulation of Connexin43. *Cardiovascular Res.* **78**, 485–493
36. Potts, J. D., and Runyan, R. B. (1989) Epithelial-mesenchymal cell transformation in the embryonic heart can be mediated, in part, by transforming growth factor β . *Dev. Biol.* **134**, 392–401
37. Rivera-Feliciano, J., Lee, K. H., Kong, S. W., Rajagopal, S., Ma, Q., Springer, Z., Izumo, S., Tabin, C. J., and Pu, W. T. (2006) Development of heart valves requires Gata4 expression in endothelial-derived cells. *Development* **133**, 3607–3618
38. Bruneau, B. G., Nemer, G., Schmitt, J. P., Charron, F., Robitaille, L., Caron, S., Conner, D. A., Gessler, M., Nemer, M., Seidman, C. E., and Seidman, J. G. (2001) A murine model of Holt-Oram syndrome defines roles of the T-box transcription factor Tbx5 in cardiogenesis and disease. *Cell* **106**, 709–721
39. Prall, O. W., Menon, M. K., Solloway, M. J., Watanabe, Y., Zaffran, S., Bajolle, F., Biben, C., McBride, J. J., Robertson, B. R., Chaulet, H., Stennard, F. A., Wise, N., Schaft, D., Wolstein, O., Furtado, M. B., Shiratori, H., Chien, K. R., Hamada, H., Black, B. L., Saga, Y., Robertson, E. J., Buckingham, M. E., and Harvey, R. P. (2007) An Nkx2–5/Bmp2/Smad1 negative feedback loop controls heart progenitor specification and proliferation. *Cell* **128**, 947–959
40. Yin, X., Wolford, C. C., Chang, Y. S., McConoughey, S. J., Ramsey, S. A., Aderem, A., and Hai, T. (2010) ATF3, an adaptive-response gene, enhances TGF β signaling and cancer-initiating cell features in breast cancer cells. *J. Cell Sci.* **123**, 3558–3565
41. Thuault, S., Valcourt, U., Petersen, M., Manfioletti, G., Heldin, C. H., and Moustakas, A. (2006) Transforming growth factor- β employs HMGA2 to elicit epithelial-mesenchymal transition. *J. Cell Biol.* **174**, 175–183
42. Thuault, S., Tan, E. J., Peinado, H., Cano, A., Heldin, C. H., and Moustakas, A. (2008) HMGA2 and Smads co-regulate SNAIL1 expression during induction of epithelial-to-mesenchymal transition. *J. Biol. Chem.* **283**, 33437–33446
43. Brandl, M., Seidler, B., Haller, F., Adamski, J., Schmid, R. M., Saur, D., and Schneider, G. (2010) IKK(α) controls canonical TGF(ss)-SMAD signaling to regulate genes expressing SNAIL and SLUG during EMT in panc1 cells. *J. Cell Sci.* **123**, 4231–4239
44. Ma, L., Lu, M. F., Schwartz, R. J., and Martin, J. F. (2005) Bmp2 is essential for cardiac cushion epithelial-mesenchymal transition and myocardial patterning. *Development* **132**, 5601–5611
45. Luna-Zurita, L., Prados, B., Grego-Bessa, J., Luxán, G., del Monte, G., Benguria, A., Adams, R. H., Pérez-Pomares, J. M., and de la Pompa, J. L. (2010) Integration of a Notch-dependent mesenchymal gene program and Bmp2-driven cell invasiveness regulates murine cardiac valve formation. *J. Clin. Invest.* **120**, 3493–3507
46. Nagarajan, R. P., Chen, F., Li, W., Vig, E., Harrington, M. A., Nakshatri, H., and Chen, Y. (2000) Repression of transforming growth factor- β -mediated transcription by nuclear factor κ B. *Biochem. J.* **348**, 591–596
47. Varelas, X., Sakuma, R., Samavarchi-Tehrani, P., Peerani, R., Rao, B. M., Dembowy, J., Yaffe, M. B., Zandstra, P. W., and Wrana, J. L. (2008) TAZ controls Smad nucleocytoplasmic shuttling and regulates human embryonic stem-cell self-renewal. *Nat. Cell Biol.* **10**, 837–848
48. Varelas, X., Samavarchi-Tehrani, P., Narimatsu, M., Weiss, A., Cockburn, K., Larsen, B. G., Rossant, J., and Wrana, J. L. (2010) The Crumbs complex couples cell density sensing to Hippo-dependent control of the TGF- β -SMAD pathway. *Dev. Cell* **19**, 831–844
49. Yagi, R., Chen, L. F., Shigesada, K., Murakami, Y., and Ito, Y. (1999) A WW domain-containing yes-associated protein (YAP) is a novel transcriptional co-activator. *EMBO J.* **18**, 2551–2562
50. Vassilev, A., Kaneko, K. J., Shu, H., Zhao, Y., and DePamphilis, M. L. (2001) TEAD/TEF transcription factors utilize the activation domain of YAP65, a Src/Yes-associated protein localized in the cytoplasm. *Genes Dev.* **15**, 1229–1241
51. Basu, S., Totty, N. F., Irwin, M. S., Sudol, M., and Downward, J. (2003) Akt phosphorylates the Yes-associated protein, YAP, to induce interaction with 14–3–3 and attenuation of p73-mediated apoptosis. *Mol. Cell* **11**, 11–23
52. Komuro, A., Nagai, M., Navin, N. E., and Sudol, M. (2003) WW domain-containing protein YAP associates with ErbB-4 and acts as a co-transcriptional activator for the carboxyl-terminal fragment of ErbB-4 that translocates to the nucleus. *J. Biol. Chem.* **278**, 33334–33341
53. Murakami, M., Nakagawa, M., Olson, E. N., and Nakagawa, O. (2005) A WW domain protein TAZ is a critical coactivator for TBX5, a transcription factor implicated in Holt-Oram syndrome. *Proc. Natl. Acad. Sci. U.S.A.* **102**, 18034–18039
54. Song, L., Zhao, M., Wu, B., Zhou, B., Wang, Q., and Jiao, K. (2011) Cell autonomous requirement of endocardial Smad4 during atrioventricular cushion development in mouse embryos. *Dev. Dyn.* **240**, 211–220